A bifunctional colchicinoid that binds to the androgen receptor

Nima Sharifi,[1,3] Ernest Hamel,[2] Markus A. Lill,[4] Prabhakar Risbood,[5] Charles T. Kane, Jr.,[6] Md Tafazzal Hossain,[6] Amanda Jones,[7] James T. Dalton,[7] and William L. Farrar[1]

[1]Cancer Stem Cell Section, Laboratory of Cancer Prevention, National Cancer Institute at Frederick, Center for Cancer Research, and [2]Toxicology and Pharmacology Branch, Developmental Therapeutics Program, Division of Cancer Treatment and Diagnosis, National Cancer Institute at Frederick, National Cancer Institute, Frederick, Maryland; [3]Medical Oncology Branch, Center for Cancer Research, National Cancer Institute, Bethesda, Maryland; [4]Department of Medicinal Chemistry and Molecular Pharmacology, Purdue University, West Lafayette, Indiana; [5]Drug Synthesis and Chemistry Branch, Division of Cancer Treatment and Diagnosis, National Cancer Institute, Rockville, Maryland; [6]Starks Associates, Inc., Buffalo, New York; and [7]Division of Pharmaceutics, College of Pharmacy, Ohio State University, Columbus, Ohio

Abstract

Castrate-resistant prostate cancer (CRPC) continues to be dependent on the androgen receptor (AR) for disease progression. We have synthesized and evaluated a novel compound that is a conjugate of colchicine and an AR antagonist (cyanonilutamide) designed to inhibit AR function in CRPC. A problem in multifunctional AR-binding compounds is steric hindrance of binding to the embedded hydrophobic AR ligand-binding pocket. Despite the bulky side chain projecting off of the AR-binding moiety, this novel conjugate of colchicine and cyanonilutamide binds to AR with a K_i of 449 nmol/L. Structural modeling of this compound in the AR ligand-binding domain using a combination of rational docking, molecular dynamics, and steered molecular dynamics simulations reveals a basis for how this compound, which has a rigid alkyne linker, is able to bind to AR. Surprisingly, we found that this compound also binds to tubulin and inhibits tubulin function to a greater degree than colchicine itself. The tubulin-inhibiting activity of this compound increases cytoplasmic AR levels in prostate cancer cells. Finally, we found that this compound has greater toxicity against androgen-independent prostate cancer cells than the combination of colchicine and nilutamide. Together, these data point to several ways of inhibiting AR function in CRPC. [Mol Cancer Ther 2007;6(8):2328–36]

Received 3/7/07; revised 5/14/07; accepted 6/15/07.

Grant support: Intramural Research Program of the NIH and the Center for Cancer Research, National Cancer Institute, and in part with Federal funds from the National Cancer Institute, NIH, under contract N02-CM-52209.

The costs of publication of this article were defrayed in part by the payment of page charges. This article must therefore be hereby marked *advertisement* in accordance with 18 U.S.C. Section 1734 solely to indicate this fact.

Requests for reprints: Nima Sharifi or William L. Farrar, Room 21-81, Cancer Stem Cell Section, Laboratory of Cancer Prevention, National Cancer Institute at Frederick, Building 560, Frederick, MD 21702. Phone: 301-451-4982; Fax: 301-846-7042. E-mail: nima.sharifi@nih.gov or farrar@ncifcrf.gov

doi:10.1158/1535-7163.MCT-07-0163

Introduction

Prostate cancer is the leading cause of nonskin malignancy in men (1). Growth and survival of prostate cancer is dependent on androgens and androgen receptor (AR) signaling. Therefore, advanced disease is generally first treated with androgen deprivation therapy by medical or surgical castration (2). Metastatic disease almost always overcomes androgen deprivation and progresses as castrate-resistant prostate cancer (CRPC). A wealth of evidence suggests that CRPC is still reliant on AR for tumor cell survival and disease progression (3). In the castrate-resistant setting, AR is reactivated by a variety of mechanisms that include but are not limited to AR gene amplification and other mechanisms of increasing AR expression and ligand-independent activation by growth factors and cytokines (4). Furthermore, a subset of androgen-responsive genes are reactivated in CRPC (5), and prostate-specific antigen declines will often occur with secondary hormonal therapies that also target AR (6). Together, this evidence suggests that AR is still a valid target in CRPC, and compounds that have novel AR-targeting mechanisms should provide new avenues for prostate cancer therapy (7).

The rationale for the design and synthesis of a compound that has independent tubulin-binding and AR-binding moieties is 4-fold. First, many tubulin-binding drugs are used for cancer chemotherapy. In fact, the only form of chemotherapy shown to prolong survival for metastatic prostate cancer patients is a tubulin-binding drug (8, 9). Addition of an AR-binding moiety to a therapeutic agent could selectively target AR-expressing prostate cancer cells, with minimal impact on cells that do not express AR. Second, the nuclear import of steroid hormone receptors is a microtubule-dependent process (10). The use of colchicine, which only binds to the soluble tubulin heterodimer and disrupts tubulin polymerization, may thereby inhibit the nuclear import of AR. Third, independent AR-binding and tubulin-binding moieties in a single compound would potentially result in concomitant AR and tubulin binding, thereby anchoring AR to tubulin. Thus, the bound AR would remain in the cytoplasm. However, a difficulty is preservation of binding to the hydrophobic AR ligand-binding domain, in which androgen ligands are completely buried (11). Adding a linker or a bulky moiety to an AR

ligand could therefore easily lead to loss of AR-binding activity. Fourth, if AR ligand-binding activity can be conserved with a compound that has a linker that extends outside the ligand-binding domain, this could disrupt binding to steroid receptor coactivators that are required for AR function (12).

Colchicine, thiocolchicine, and combretastatin A-4 all bind to a common site on tubulin referred to as the colchicine site (13). Studies of the structure-activity relationship of colchicine suggest that the C7 acetamido group can be modified while preserving tubulin-binding activity (14). We therefore chose this site for one end of the linker. Cogan and Koch (15) used a rigid alkyne linker with a cleavable salicylamide *N*-Mannich base in doxorubicin-targeting for prostate cancer. Although we used the alkyne moiety, we excluded the salicylamide *N*-Mannich base and selected a noncleavable linker to allow for the possibility of concomitant AR and tubulin binding. We constructed a linker with sufficient length to extend the colchicine moiety outside the AR ligand-binding domain. Cyanonilutamide is structurally similar to nilutamide and has a slightly higher affinity for the AR than does nilutamide (15).

These considerations led us to synthesize acetamide, 2-[4-[3-[(4-cyano-3-trifluoro-methyl)phenyl]-5,5-dimethyl-2,4-dioxoimidazol-idin-1-yl]-but-2-ynyloxy]-*N*-[(7*S*)-5,6,7,9-tetrahydro-1,2,3,10-tetramethoxy-9-oxobenzo[*a*]heptalen-7-yl], and will hereafter refer to this compound as CCN, for colchicine-cyanonilutamide. Here, we describe the properties of CCN and the structural basis for how it binds AR. CCN binds to tubulin and inhibits tubulin assembly with greater potency than colchicine and has activity that is comparable to the more potent thiocolchicine (13). Despite the hydrophobic binding pocket of the AR ligand-binding domain and the relatively bulky nature of colchicine, CCN still retains AR-binding activity. We determined the structural basis of binding to the AR ligand-binding domain using molecular modeling techniques. We found that the alkyne-based linker allows for a sufficient distance between the cyanonilutamide and colchicine moieties to allow the former to bind in the binding pocket and at the same time for the latter to extend outside AR. Furthermore, we found that colchicine and CCN increase cytoplasmic AR protein levels in prostate cancer cells. Moreover, we found that CCN is more potent in killing androgen-independent prostate cancer cells than colchicine as well as the combination of colchicine and nilutamide. Together, this work provides several insights that could be used in further modifications for the design of compounds to be used for the treatment of advanced, incurable CRPC.

Materials and Methods

Chemistry

^{1}H nuclear magnetic resonance (^{1}H NMR) spectra were recorded at 400, 500, or 600 MHz, and signals are given in parts per million. *J* values are given in Hertz. Mass spectra were determined by electrospray. Column chromatography was carried out using Merck 60 silica gel (70–230 mesh). TLC was done on Merck 60 F_{254} silica gel glass plates. Elemental analyses were done by Atlantic Microlabs. Melting points are uncorrected. Unless stated, all solvents and reagents were purchased from commercial sources and used without further purification.

Benzonitrile, 4-[3-(4-Hydroxy-2-Butynyl)-4,4-Dimethyl-2,5-Dioxo-1-Imidazolidinyl]-2-(Trifluoromethyl)- (2). To **1** (ref. 15; 3.90 g, 13.1 mmol) in dimethylformamide (DMF; 60.0 mL) was added cesium carbonate (3.85 g, 11.8 mmol) and a solution of 4-chloro-2-butyn-1-ol (3.60 g, 34.4 mmol) in DMF (5.0 mL). After 3 h at room temperature, the mixture was filtered. The filtrate was diluted with EtOAc (500 mL), washed with water (1.2 L), then dried ($MgSO_4$) and concentrated. The white solid was dried under reduced pressure to give **2** (2.85 g, 59%). ^{1}H NMR (500 MHz, DMSO-d_6): δ 8.32 (d, 1H, *J* = 8.4 Hz); 8.20 (d, 1H, *J* = 1.6 Hz); 8.06–8.04 (dd, 1H, *J* = 1.7, 8.4 Hz); 5.16–5.14 (t, 1H, *J* = 5.9 Hz); 4.30 (s, 2H); 4.08–4.07 (m, 2H); 1.54 (s, 6H). Mass spectroscopy: electrospray (positive ion): calculated for $C_{17}H_{14}F_3N_3O_3$ = 365; found: *m/z* (relative intensity) 383 [$(M + NH_4)^+$, 100%]. HPLC: retention time 13.879 min with 100% peak area [Luna C18, 4.6 × 250 mm, 5 μ. Mobile phase: A = 0.05 mol/L H_3PO_4 buffer (pH, 3); B = acetonitrile + 1% water. Linear gradient = 95% A; 70% A; 100% B; 95% A].

Acetic Acid, 2-[4-[3-[(4-Cyano-3-Trifluoromethyl)-Phenyl]-5,5-Dimethyl-2,4-Dioxoimidazolidin-1-yl]But-2-ynyloxy]-Methyl Ester (3). A mixture of **2** (1.80 g, 4.93 mmol) and thallium ethoxide (349 μL, 4.93 mmol) in CH_3CN (17.0 mL) was stirred for 1 h at ambient temperature and then concentrated to dryness. The powder was dissolved in DMF (17.0 mL), and methyl bromoacetate (3.8 g, 24.8 mmol) was added. The mixture was heated at 60°C for 3 h and then cooled to room temperature, and water (50 mL) was added. This was extracted with diethyl ether (4 × 100 mL), dried ($MgSO_4$), and concentrated. The crude product was purified by column chromatography (silica gel, hexanes/EtOAc, 1:1) to give **3** (920 mg, 43%), melting point 73 to 75°C (uncorrected). Elemental analysis: calc.: C(61.30), H(5.35), N(7.01); found: C(61.26), H(5.34), N(6.88). ^{1}H NMR (400 MHz, DMSO-d_6): δ 8.33–8.31 (d, 1H, *J* = 8.4 Hz); 8.19 (s, 1H); 8.04–8.02 (dd, 1H, *J* = 1.5, 8.0 Hz); 4.33 (s, 2H); 4.25 (s, 2H); 4.16 (s, 2H); 3.63 (s, 3H); 1.52 (s, 6H). Mass spectroscopy: electrospray (positive ion): calculated for $C_{20}H_{18}F_3N_3O_5$ = 437; found: *m/z* (relative intensity) 460 [$(M + Na)^+$, 100%]. TLC (silica gel, E. Merck 60 F-254 glass plates): R_f value = 0.42 (EtOAc/hexanes, 1:1).

Acetic Acid, 2-[4-[3-[(4-Cyano-3-Trifluoromethyl)-Phenyl]-5,5-Dimethyl-2,4-Dioxoimidazolidin-1-yl]But-2-ynyloxy]- (4). A cold solution of **3** (500 mg, 1.14 mmol) and 1.0 mol/L NaOH (1.178 mL, 1.178 mmol) in methanol (7.50 mL) was stirred at room temperature for 2.5 h. The reaction mixture was diluted with water (50 mL) and extracted with EtOAc (3 × 100 mL). The aqueous layer was acidified to pH 2 (1 N HCl) and extracted with CH_2Cl_2 (4 × 100 mL). The combined organic layer was washed with water (3 × 100 mL) and brine (100 mL), then dried (Na_2SO_4), and concentrated to give **4** (231 mg, 48%). ^{1}H NMR (500 MHz,

DMSO-d_6): δ 12.69 (s, 1H); 8.32–8.30 (d, 1H, J = 8.4 Hz); 8.20 (d, 1H, J = 1.3 Hz); 8.06–8.04 (dd, 1H, J = 1.5, 8.4 Hz); 4.34 (s, 2H); 4.26 (s, 2H); 4.05 (s, 2H); 1.54 (s, 6H). Mass spectroscopy: electrospray (negative ion) calculated for $C_{19}H_{16}F_3N_3O_5$ = 423; found: *m/z* (relative intensity) 422 [$(M-H)^-$,100%].

Acetamide, 2-[4-[3-[(4-Cyano-3-Trifluoromethyl)-Phenyl]-5,5-Dimethyl-2,4-Dioxo-Imidazolidin-1-yl]-But-2-ynyloxy]-*N*-[(7*S*)-5,6,7,9-Tetrahydro-1,2,3,10-Tetramethoxy-9-Oxobenzo[*a*]heptalen-7-yl]- (6). To a solution of **5** (ref. 16; 175 mg, 0.490 mmol) and 4-methylmorpholine (176 μL, 1.60 mmol) in $CHCl_3$ (6.0 mL) was added a solution of **4** (226 mg, 0.534 mmol) in $CHCl_3$ (3.0 mL) and (benzotriazol-1-yloxy)tris-(dimethylamino)phosphonium hexafluorophosphate (BOP; 590 mg, 1.33 mmol). After 3.5 h at room temperature, the reaction mixture was diluted with $CHCl_3$ (150 mL) and washed with saturated aqueous citric acid (3 × 50 mL). The organic layer was concentrated to dryness, and the crude product was purified by column chromatography (silica gel, EtOAc/methanol, 19:1) to give **6** (220 mg, 60%) as an orange solid. Elemental analysis: calculated for $C_{39}H_{37}F_3N_4O_9 \cdot 0.3$ hexanes$\cdot 0.6$ H_2O: C(61.30), H(5.35), N(7.01); found: C(61.26), H(5.34), N(6.88). ^{1}H NMR (600 MHz, DMSO-d_6): δ 8.59–8.57 (d, 1H, J = 7.6 Hz); 8.32–8.31 (d, 1H, J = 8.4 Hz); 8.20–8.19 (d, 1H, J = 1.3 Hz); 8.05–8.03 (dd, 1H, J = 1.5, 8.4 Hz); 7.13 (s, 1H); 7.11–7.01 (dd, 2H, J = 10.6, 50.2 Hz); 6.76 (s, 1H); 4.41–4.37 (m, 1H); 4.35 (s, 2H); 4.27 (s, 2H); 3.98–3.92 (dd, 2H, J = 14.9, 20.1 Hz); 3.86 (s, 3H); 3.83 (s, 3H); 3.78 (s, 3H); 3.52 (s, 3H); 2.60–2.56 (dd, 1H, J = 6.0, 13.1 Hz); 2.23–2.18 (m, 1H); 2.04–1.93 (m, 2H); 1.51 (s, 6H). Mass spectroscopy: electrospray (positive ion): calculated for $C_{39}H_{37}F_3N_4O_9$ = 762; found: *m/z* (relative intensity) 763 [$(M + H)^+$,100%]. TLC (silica gel, E. Merck 60 F-254 glass plates): R_f value = 0.27 (EtOAc/methanol, 19:1).

Molecular Modeling of CCN Bound to AR

Protein Structure. Molecular modeling was based on the high-resolution structure (1.65 Å resolution) of human wild-type AR complexed with the agonist R-3 (PDB-code: 2AX9; ref. 17); a structure for apo-AR and AR with an antagonist bound has not yet been determined. The X-ray structures of rat AR with BMS-564929 (2NW4; ref. 18), a compound similar to cyanonilutamide, was resolved to only 3 Å. We aligned 2NW4 onto 2AX9. Based on the conformational differences in their ligand-binding site, we modified the side chains of Asn^{705}, Gln^{711}, and Met^{895} in 2AX9 allowing to accommodate cyanonilutamide. Missing loop residues 844 to 851 were added using the loopy v1.0 (19) module from the Jackal 1.5 suite (Columbia University).

Preparation of Molecular Dynamics (MD) Simulations. All molecular dynamics (MD) simulations were done with Gromacs 3.1 (20) using the Gromos 53A6 force field. The ligands were built and prepared for MD simulations using Maestro (Schrödinger, LLC) and PRODRG (21). A solvent box (including counterions) with at least 10 Å distance from box wall to any solute atom was added around the ligand-protein complex (~37,500 atoms in total). All simulations were done with a generalized reaction field and a dual group cutoff of 8 and 14 Å. Equilibration was done using a NpT-ensemble, whereas steered MD (SMD) simulations were run under NVT-conditions. A time step of 2 fs was chosen using the LINCS algorithm for constraining bonds.

SMD. In SMD, an *in silico* model for AFM experiments (22), a spring was attached to the ethyl group of cyanonilutamide ethylated at the 3-position of the 5,5-dimethyl-2,4-dioxoimidazol-idin-1-yl portion. This ethyl group functions as starting elements of the linker and was initially oriented toward three channels. These paths were visually identified in the X-ray structure as possible channels (with similar dimension as the length of the linker) through which the hydrophobic linker could be topologically positioned when CCN binds to AR. The spring moves with constant velocity v along a predefined direction $\vec{v}$. As the movement of the ligand along this direction experiences resistance, the spring is stretched, which results in external force $F = k(vt - x)$ that the ligand is experiencing. Simulations with different force constants k ranging from 500 to 10,000 kJ mol^{-1} nm^{-2} and pulling velocities v ranging from 2 to 5 nm ns^{-1} were done. We finally chose k = 500 kJ mol^{-1} nm^{-2} and v = 3 nm ns^{-1}, the same values as in a previous study on the thyroid receptor (11). This allows us to compare the resulting force profiles $F(t)$ of ligands dissociating from two different species of the nuclear receptor family. For each channel, the protein ligand complex was equilibrated for 1.5 ns (0.5 ns solvent equilibration only). Seven SMD simulations (1 ns each) along each of the channels were run with slightly modified directions.

Equilibration of the AR-CCN Complex. For channels I and II, the linker was grown into the channel in three steps, always merging between two and four additional heavy atoms to cyanonilutamide. The resulting new structure was equilibrated using 2,500 steps of steepest descent energy minimization and 1 ns of MD simulations before the linker was elongated any further. Finally, the colchicine moiety was attached to the cyanonilutamide-linker compound, and the full system was equilibrated using a 10-ns MD simulation.

Tubulin Assembly and Tubulin Binding Studies

Inhibition of tubulin assembly (23) and inhibition of colchicine binding (24) were measured as described in detail previously. In the assembly reaction, 10 μmol/L tubulin was used. In the colchicine binding reaction, tubulin was at 1.0 μmol/L and both [^{3}H]colchicine and the inhibitor at 5 μmol/L. Combretastatin A-4 was generously provided by Dr. G.R. Pettit (Arizona State University, Tempe, AZ), and thiocolchicine was provided by Dr. A. Brossi (National Institute of Diabetes and Digestive and Kidney Diseases, Bethesda, MD). Colchicine was purchased from Sigma.

Tritiated Mibolerone Binding Studies

The AR-binding affinity of synthetic AR ligands was determined using an *in vitro* radioligand competitive binding assay as previously described (25). Briefly, an aliquot of AR cytosol isolated from the ventral prostates of castrated male rats was incubated with 1 nmol/L of [^{3}H]mibolerone and 1 mmol/L of triamcinolone acetonide

at 4°C for 18 h in the absence or presence of 10 increasing concentrations of CCN (10^{-1} to 10^4 nmol/L). Nonspecific binding of [^{3}H]mibolerone was determined by adding excess unlabeled mibolerone (1,000 nmol/L) to the incubate in separate tubes. After incubation, the AR-bound radioactivity was isolated using the hydroxyapatite (HAP) method (25). The bound radioactivity was then extracted from HAP and counted. The specific binding of [^{3}H]mibolerone at each concentration of the compound of interest was calculated by subtracting the nonspecific binding of [^{3}H]mibobolerone and expressed as the percentage of the specific binding in the absence of the compound of interest (B0). The concentration of CCN that reduced B0 by 50% (i.e., IC_{50}) was determined using WinNonlin (Pharsight Corporation). The equilibrium binding constant (K_i) of the compound of interest was calculated by $K_i = K_d\ IC_{50}/(K_d + L)$, where K_d was the dissociation constant of [^{3}H]mibolerone (0.19 ± 0.01 nmol/L), and L was the concentration of [^{3}H]miboleerone used in the experiment (1 nmol/L). The K_i value of each compound of interested was further compared.

Cell Culture, Cell Survival Assay, and Western Blots

LNCaP cells were grown in RPMI 1640 supplemented with 10% fetal bovine serum and glutamine. Cells were exposed to vehicle, 0.1 μmol/L nilutamide, 0.1 μmol/L colchicine, and 0.1 μmol/L CCN for 11 h, and cells were washed with PBS. Protein was cross-linked *in situ* by treating with 1 mmol/L dithiobis(succinimidyl)propionate (DSP; Pierce) for 30 min at room temperature and gently rocked. Excess DSP was neutralized with 1 mol/L Tris (pH, 7.5). Nuclear and cytoplasmic protein extracts were prepared using the Pierce nuclear and cytoplasmic fractionation kit. Exactly 40 μg protein was analyzed on a 4% to 20% Tris-glycine gel, and protein was transferred to a polyvinylidene fluoride membrane, blocked in 1% fish gelatin in PBS, incubated sequentially with rabbit anti-AR antibody (Cell Signaling) and a horseradish peroxidase–labeled anti-rabbit secondary antibody (Amersham, GE Healthcare) using standard methods. Membranes were then incubated with horseradish peroxidase substrate solution (Amersham) before exposure to film. LAPC4AI cells were obtained courtesy of Dr. Charles Sawyers and grown in IMEM supplemented with 10% fetal bovine serum and glutamine. Cells were plated at 50,000 cells per well on a 96-well plate. The following day, 0.01, 0.05, and 0.1 μmol/L colchicine and CCN were added to cells, in addition to the combination of 0.05 μmol/L colchicine and 0.05 μmol/L nilutamide, all in triplicate. After 48 h of incubation, cell survival was measured with the CellTiter-Blue assay (Promega), as specified by the manufacturer.

Results

Linking the C7 acetamido group of colchicine through an alkyne linker to cyanonilutamide results in CCN. Cyanonilutamide is a derivative of the AR antagonist nilutamide, which is in clinical use for prostate cancer. Combretastatin A-4 and thiocolchicine are structurally related to colchicine and also bind at the tubulin colchicine site. CCN was designed as a bifunctional compound that would interact with both tubulin and AR. All structures are shown in Fig. 1A.

Compound **1** was prepared by the method of Cogan and Koch (ref. 15; Fig. 1B). Alkylation of **1** with 4-chloro-2-butyn-1-ol gives alcohol **2**. Alkylation of the thallium salt of **2**, followed by hydrolysis, gives carboxylic acid **4**. Intermediate **5** was prepared in three steps using the method of Bagnato et al. (16). BOP coupling of **4** and **5** gives the compound **6** (CCN) in 60% yield.

As a first step to evaluate CCN, we sought to determine AR-binding activity. Tritiated mibolerone binding studies of CCN showed that the K_i of this compound is 449 ± 49 nmol/L, and in the same experiments, the K_i of dihydrotestosterone is 0.2 to 0.3 nmol/L. Hydroxyflutamide, which is the active metabolite of flutamide, a clinically used AR antagonist, has a K_i of about 50 nmol/L (26). Therefore, despite the bulky colchicine side chain, CCN binds AR with only a 1 log lower affinity than a clinically active AR antagonist. The AR-binding activity of CCN suggests that the rigid alkyne linker functions as designed to extend the colchicine moiety outside the enclosed hydrophobic AR ligand-binding pocket with preservation of the AR-binding activity of cyanonilutamide.

To investigate the structural basis of CCN binding to AR, we employed molecular modeling techniques based on known X-ray structures of AR-ligand complexes. Visual inspection of the modified AR X-ray structure (see Materials and Methods) with a compound structurally similar to cyanonilutamide (BMS-564929) revealed three small channels of appropriate length for the linker to extend the colchicine moiety outside of the AR ligand-binding domain. Channel I is composed of the region between helices 3, 6, 7, and 11; channel II is composed of the region between helices 11 and 12; and channel III is the mobile region between helices 1 and 2 as well as helices 3 and 5. Topological feasibility of a channel to accommodate the linker region of CCN is a necessary, but not sufficient, property for binding. The channel must also allow the cyanonilutamide portion of the compound to enter and exit the hydrophobic binding pocket of AR. To address this issue, we did SMD simulations of cyanonilutamide ethylated at the 3-position of the 5,5-dimethyl-2,4-dioxoimidazol-idin-1-yl portion, pulling the ethyl group along the three channels (Table 1).

Although SMD along channel I yields the highest maximum force, none of the paths is statistically favored over the others, taking the SD of ~30 to 50 pN over seven simulations along each path into account. Considering the integrated force, i.e., the total work done (with a SD of about 20 pN ns), paths I and II are energetically favored over path III, and these values are lower than comparable values for the thyroid receptor (11). Consequently, we docked CCN in two different binding modes, with its linker bound within channel I or II.

Standard MD equilibration simulations of CCN with its linker bound within channel I (Fig. 2A) showed that this configuration of binding occurs without substantial

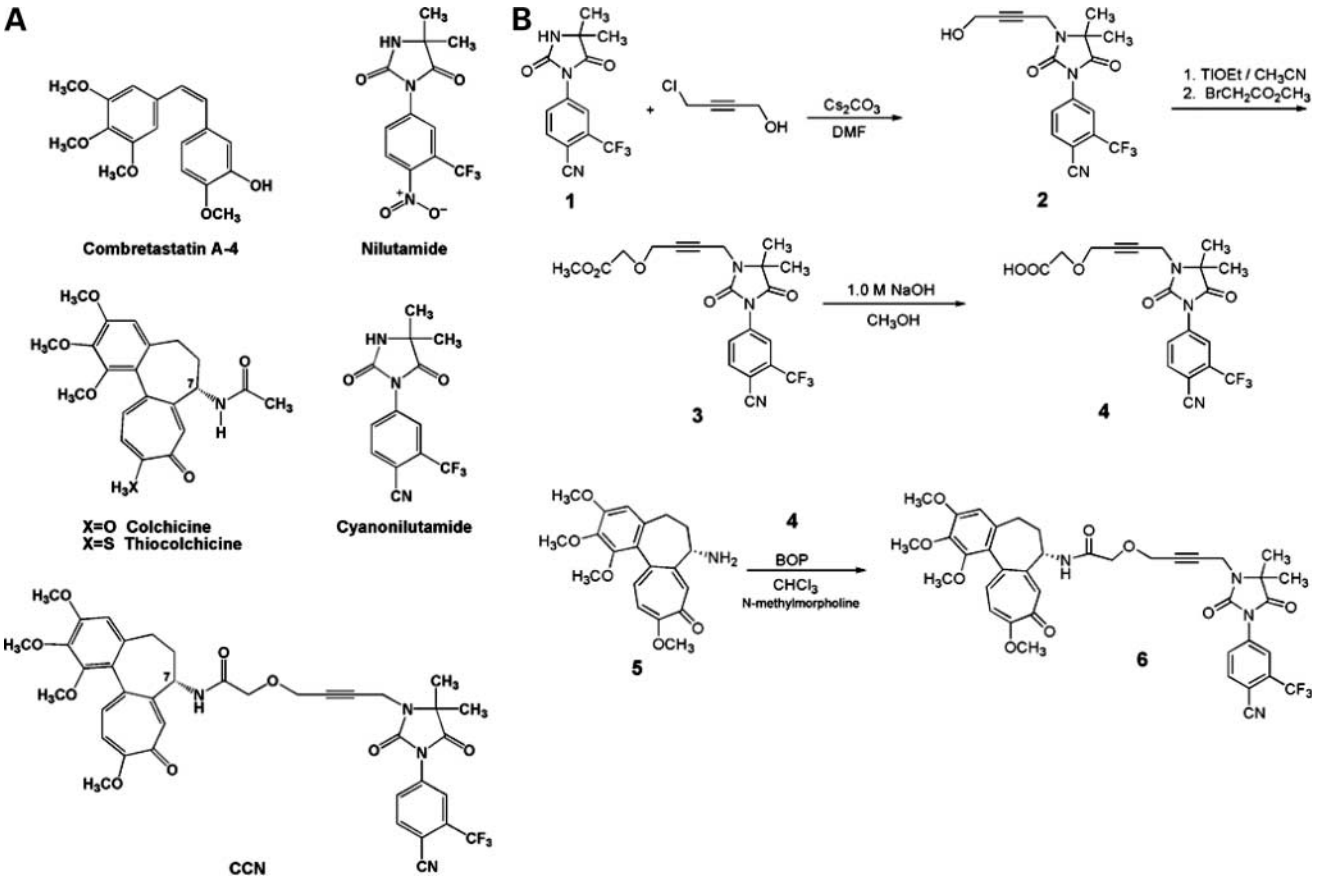

Figure 1. **A,** structures of combretastatin A-4, colchicine, thiocolchicine, nilutamide, cyanonilutamide, and CCN. **B,** synthesis of CCN.

conformational changes in the protein. The length and hydrophobic character of the channel are perfectly suited for the predominantly hydrophobic linker, such that cyanonilutamide binds in the binding pocket of AR, and the colchicine moiety resides outside the AR ligand-binding domain. After 10 ns equilibration, a conformational change in helix 12 and the COOH terminus of helix 11 was observed, whereas the other portions of helices comprising channel I remained almost unaltered. We can only speculate if the observed change in helix 11, and especially in helix 12, might reflect an antagonistic effect on AR (similar to the conformational changes observed in estrogen receptor, for example; ref. 27); no experimental X-ray structure of wild-type AR with an antagonist has yet been determined.

MD simulations of CCN binding to AR, with the linker positioned in channel II (Fig. 2B), results in a significant conformational change in helix 11. However, we should mention that according to the proposed mouse-trap model (28) for ligand association with nuclear receptors, the conformations of helices 11 and 12 might differ from the X-ray structures used as starting points for our simulations. Due to the lack of experimental structural information of Apo or antagonist structures for AR, these scenarios cannot be ruled out.

There are extensive structure-activity relationship data for colchicine in the literature (13). Furthermore, the colchicine binding site on tubulin has been defined by X-ray crystallography (29). Although the colchicine binding site is primarily in the β-subunit of tubulin, the drug binds close to the intradimer α-β interface (29). Thus, colchicine analogues also interact with the tubulin α-subunit (13). Colchicine only binds to the soluble tubulin heterodimer and induces a conformational change, thereby inhibiting tubulin polymerization (13). We found that CCN inhibited tubulin assembly with an IC_{50} of 1.1 ± 0.1 μmol/L and is a better inhibitor of tubulin assembly than colchicine itself (Table 2). CCN was also examined for its ability to inhibit the binding of [^{3}H]colchicine to tubulin, in comparison with thiocolchicine and combretastatin A-4. Inhibitory

Table 1. Maximum and integrated force of the average force profiles

Path	Maximum force (pN)	Integrated force (pN ns)
I	629	259
II	589	266
III	584	379

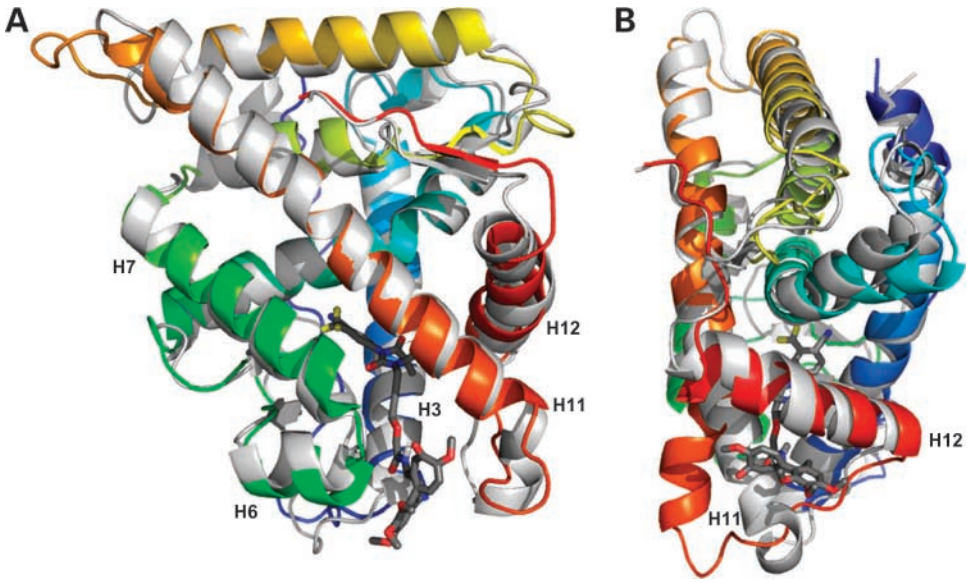

Figure 2. Representation of two possible modes of CCN binding to the AR after MD equilibration. **A,** binding occurs along channel I, which is the path between helices 3, 6, 7, and 11. **B,** binding occurs in the path along channel II, which resides between helices 11 and 12. *Gray,* X-ray structure.

effects on tubulin assembly and on colchicine binding were equivalent to those of thiocolchicine (Table 2). In comparison with combretastatin A-4, CCN was a more effective inhibitor of assembly, but it was less potent as an inhibitor of [^{3}H]colchicine binding. This potent inhibition of colchicine binding by combretastatin A-4 derives entirely from its rapid binding to tubulin, in comparison with the slower binding of colchicinoids (30). Given the increased activity of CCN over colchicine and the fact that some steroid receptor ligands have tubulin-binding activity (31), we verified that cyanonilutamide had no effect on tubulin assembly (data not shown).

We then examined how CCN affects AR localization. LNCaP prostate cancer cells have a mutation in the AR ligand-binding domain, which changes the antagonist activity of some clinically used prostate cancer drugs to agonist activity (32). This sort of change may account for the antiandrogen withdrawal phenomenon seen in some patients (33). Therefore, any effect of CCN on AR cellular localization, although it may be related to AR binding, should not be related to classic antagonist activity. LNCaP cells have both nuclear and cytoplasmic AR without stimulation. We found that treatment with 0.1 μmol/L CCN or 0.1 μmol/L colchicine increased cytoplasmic AR protein levels without a detectable change in nuclear AR (Fig. 3). Treatment with 0.1 μmol/L nilutamide decreased cytoplasmic AR and increased nuclear AR, as would be expected with nuclear import. The increase in cytoplasmic AR upon treatment with CCN or colchicine is most likely related to tubulin depolymerization and the inability of dyenin- and microtubule-dependent steroid receptor nuclear import to occur.

Next, we tested the effect of CCN on the growth of the androgen-independent LAPC4AI cell line. Cells were treated with CCN, colchicine, and a combination of colchicine and nilutamide for 48 h (Fig. 4). We found that CCN inhibits androgen-independent cell survival more than colchicine, with a difference that is maximal at 0.05 μmol/L. To rule out the possibility that the cell toxicity of CCN is reproducible with a combination of colchicine and an AR antagonist, LAPC4AI cells were also treated with a combination of 0.05 μmol/L colchicine and 0.05 μmol/L nilutamide. This combination resulted in toxicity that is the same as 0.05 μmol/L colchicine alone.

Discussion

Advanced CRPC remains an incurable disease. A spectrum of clinical, biochemical, and genetic data point to AR as a valid target, even in prostate cancer that progresses in the face of testosterone depletion (3, 4, 7). Here, we have synthesized and characterized CCN, a compound designed to antagonize AR function in a novel manner. Cogan and Koch (15) used a cleavable alkyne linker to target doxorubicin to AR-positive cells. We have used a non-cleavable alkyne linker to add an additional functional moiety to an AR ligand for novel AR antagonism. We have shown that this compound has several important properties

Table 2. Inhibitory effects of CCN, colchicine, thiocolchicine, and combretastatin A-4 on tubulin assembly and on binding of [^{3}H]colchicine to tubulin

Compound	Inhibition of tubulin assembly IC_{50} (μmol/L), mean ± SD	Inhibition of [^{3}H]colchicine binding (%), mean ± SD
Colchicine-cyanonilutamide	1.1 ± 0.1	64 ± 1
Thiocolchicine	1.0 ± 0.1	67 ± 0.07
Colchicine	2.2 ± 0.4	—
Combretastatin A-4	1.3 ± 0.08	98 ± 0.6

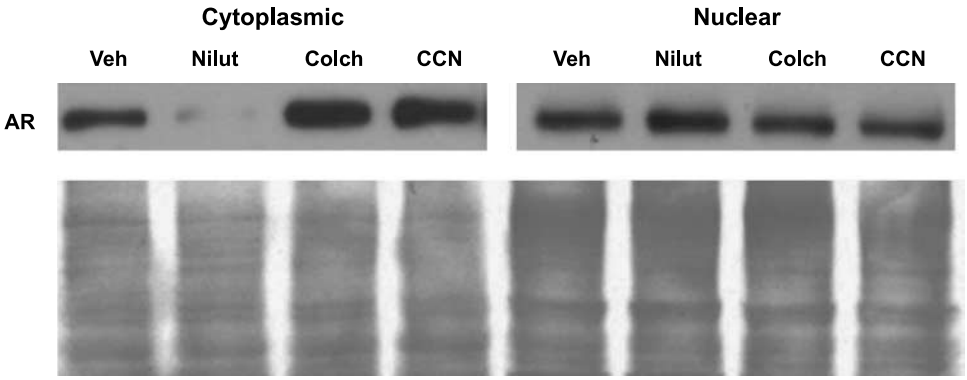

Figure 3. Colchicine and CCN increase cytoplasmic AR protein levels without a detectable change in nuclear AR. Western blots of nuclear and cytoplasmic LNCaP extracts are shown after 11 h of exposure to vehicle (*Veh*), 0.1 μmol/L nilutamide (*Nilut*), 0.1 μmol/L colchicine (*Colch*), or 0.1 μmol/L CCN (*CCN*). Ponceau S–stained membrane is shown for protein loading control.

that can be exploited in the design of other compounds for novel mechanisms of AR antagonism.

As shown here, a single compound can have both functional AR-binding and tubulin-binding activities with independent moieties. Steroid ligands, including testosterone and dihydrotestosterone, are hydrophobic hormones. Hence, they readily bind in their complementary hydrophobic receptor ligand-binding pockets. An issue in designing a bifunctional compound that binds to any steroid hormone receptor, including AR, is accessibility to such a hydrophobic pocket in the ligand-binding domain. Despite the potential for steric hindrance, CCN retains reasonable binding activity for AR. This indicates that the linker in CCN must project the colchicine moiety out of the ligand-binding domain to maintain AR binding.

Molecular modeling of CCN in the binding pocket of AR indicates three potential channels through which linker length is consistent with AR binding. SMD shows that although the highest maximum force is along channel I, statistically, there is no significant difference among channels I, II, and III. However, when the integrated force is taken into account, we found that the paths along channels I and II are the most energetically favored among the three possibilities. The hydrophobicity and length of channel I, which is encompassed by helices 3, 6, 7, and 11, and the need for only minimal conformational changes in the protein make this path seem appropriately suited to accommodate CCN. Accommodation of CCN into channel II would require more significant conformational changes. However, given the proposed changes in helices 11 and 12 in the mouse-trap model for ligand binding to steroid hormone receptors, the starting positions of the helices in this model may not be fully representative. We cannot eliminate the possibility of either channel I or channel II in accommodating the alkyne linker to allow the colchicine moiety to reside outside the ligand-binding domain. Both of these paths could explain the AR-binding activity of CCN.

CCN is derived by linking the colchicine C7 acetamido group to cyanonilutamide. It is intriguing that this compound is a more potent inhibitor of tubulin assembly than colchicine or combretastatin A-4 and has activity that is similar to that of thiocolchicine. Although there is the possibility that some substitutions at the C7 position of colchicine have activity that is independent of the tubulin colchicine site (13), we found that CCN inhibition of [^{3}H]colchicine binding parallels its inhibition of tubulin assembly activity and suggests that it works through the tubulin colchicine site.

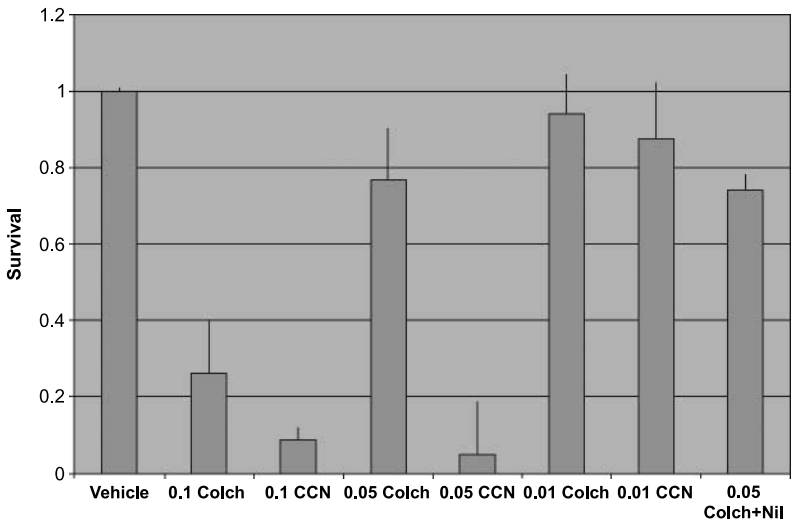

Figure 4. CCN is more toxic to androgen-independent LAPC4AI cells than colchicine and the combination of colchicine and nilutamide. LAPC4AI cells were plated in triplicate, exposed to CCN, colchicine, or a combination of colchicine and nilutamide the following day. Compound concentrations are in micromolar. Cell survival was measured with the CellTiter-Blue assay after 48 h. *Bars,* 1 SD from the mean.

Although one of our intents in the design and synthesis of CCN was to have independent moieties that bind AR and tubulin concomitantly, in an attempt to anchor AR to the cytoplasm, we were unable to show concomitant binding by either *in situ* protein cross-linking in LNCaP cells and immunoprecipitation or with purified tubulin and GST-LBD coincubation and GST pulldown (data not shown). This may relate to the relative positions of AR and tubulin and steric inhibition of one protein binding CCN by the other concomitantly. Nevertheless, the functional activities of both moieties of CCN, as well as the modeling of how the noncleavable alkyne linker permits AR binding of the cyanonilutamide moiety and at the same time projects the tubulin-binding moiety outside AR, may serve as a basis for the design of further bifunctional AR ligands that may be able to show concomitant AR and tubulin binding. More broadly, our findings may serve as a basis for other bifunctional steroid receptor ligands.

Exposure of LNCaP prostate cancer cells to either colchicine or CCN increases cytoplasmic AR levels. This most likely occurs through the inhibition of microtubule formation and, consequently, dynein-dependent steroid hormone transport along microtubules to the nucleus (10). However, we did not observe any discernible decrease in nuclear AR levels. The increased cytoplasmic AR without detectable decrease in nuclear AR may relate to the relative concentration of AR in each cellular compartment. A small decrease in nuclear AR where the AR concentration is higher is probably a more subtle finding. Therefore, we cannot rule out small changes in nuclear AR on exposure to colchicine or CCN. Inhibition of tubulin-dependent AR nuclear import could be exploited to antagonize AR function in CRPC.

CCN is more toxic to androgen-independent LAPC4AI cells than colchicine. In addition, the combination of colchicine and nilutamide is no more toxic than colchicine alone. This suggests that the activity of CCN is not due to the synergy of the individual activities of colchicine and the AR antagonist moiety of CCN and, therefore, must be due to a property that is unique to CCN. However, given that CCN is a more potent inhibitor of tubulin assembly than colchicine, we cannot eliminate the possibility that the greater toxicity of CCN is, in part, due to enhanced inhibition of tubulin assembly.

In conclusion, we have described the design, synthesis, and the activities of CCN. This novel compound has retained AR-binding activity and more potent tubulin-binding and inhibition of tubulin polymerization activity than colchicine itself. Furthermore, molecular modeling of CCN suggests two paths through which binding to AR is structurally and energetically feasible, explaining its AR-binding activity. The antitubulin activity of CCN increases cytoplasmic AR protein levels, where AR is inactive. Lastly, CCN is more toxic to androgen-independent prostate cancer cells than the combination of its tubulin-binding parent drug and nilutamide. Together, these data provide insights into the possibility of using bifunctional AR ligands to antagonize AR activity in CRPC. Our findings with CCN may be useful in the design of other bifunctional steroid receptor ligands.

Acknowledgments

We thank Tad Koch (University of Colorado) for discussions related to linker modification and design, Susan Bane (State University of New York at Binghampton) for discussions on the structure-activity relationship of colchicine, and Charles Sawyers for provision of LAPC4AI cells.

References

1. Jemal A, Siegel R, Ward E, Murray T, Xu J, Thun MJ. Cancer statistics, 2007. CA Cancer J Clin 2007;57:43 – 66.

2. Sharifi N, Gulley JL, Dahut WL. Androgen deprivation therapy for prostate cancer. JAMA 2005;294:238 – 44.

3. Scher HI, Sawyers CL. Biology of progressive, castration-resistant prostate cancer: directed therapies targeting the androgen-receptor signaling axis. J Clin Oncol 2005;23:8253 – 61.

4. Heinlein CA, Chang C. Androgen receptor in prostate cancer. Endocr Rev 2004;25:276 – 308.

5. Holzbeierlein J, Lal P, LaTulippe E, et al. Gene expression analysis of human prostate carcinoma during hormonal therapy identifies androgen-responsive genes and mechanisms of therapy resistance. Am J Pathol 2004;164:217 – 27.

6. Small EJ, Ryan CJ. The case for secondary hormonal therapies in the chemotherapy age. J Urol 2006;176:S66 – 71.

7. Sharifi N, Farrar WL. Androgen receptor as a therapeutic target for androgen independent prostate cancer. Am J Ther 2006;13:166 – 70.

8. Petrylak DP, Tangen CM, Hussain MH, et al. Docetaxel and estramustine compared with mitoxantrone and prednisone for advanced refractory prostate cancer. N Engl J Med 2004;351:1513 – 20.

9. Tannock IF, de Wit R, Berry WR, et al. Docetaxel plus prednisone or mitoxantrone plus prednisone for advanced prostate cancer. N Engl J Med 2004;351:1502 – 12.

10. Harrell JM, Murphy PJ, Morishima Y, et al. Evidence for glucocorticoid receptor transport on microtubules by dynein. J Biol Chem 2004;279:54647 – 54.

11. Martinez L, Webb P, Polikarpov I, Skaf MS. Molecular dynamics simulations of ligand dissociation from thyroid hormone receptors: evidence of the likeliest escape pathway and its implications for the design of novel ligands. J Med Chem 2006;49:23 – 6.

12. Estebanez-Perpina E, Moore JM, Mar E, et al. The molecular mechanisms of coactivator utilization in ligand-dependent transactivation by the androgen receptor. J Biol Chem 2005;280:8060 – 8.

13. Hastie SB. Interactions of colchicine with tubulin. Pharmacol Ther 1991;51:377 – 401.

14. Berg U, Deinum J, Lincoln P, Kvassman J. Stereochemistry of colchicinoids. Enantiomeric stability and binding to tubulin of desacetamidocolchicine and desacetamidoisocolchicine. Bioorg Chem 1991;19:53 – 65.

15. Cogan PS, Koch TH. Rational design and synthesis of androgen receptor-targeted nonsteroidal anti-androgen ligands for the tumor-specific delivery of a doxorubicin-formaldehyde conjugate. J Med Chem 2003;46:5258 – 70.

16. Bagnato JD, Eilers AL, Horton RA, Grissom CB. Synthesis and characterization of a cobalamin-colchicine conjugate as a novel tumor-targeted cytotoxin. J Org Chem 2004;69:8987 – 96.

17. Bohl CE, Miller DD, Chen J, Bell CE, Dalton JT. Structural basis for accommodation of nonsteroidal ligands in the androgen receptor. J Biol Chem 2005;280:37747 – 54.

18. Ostrowski J, Kuhns JE, Lupisella JA, et al. Pharmacological and X-ray structural characterization of a novel selective androgen receptor modulator: potent hyperanabolic stimulation of skeletal muscle with hypostimulation of prostate in rats. Endocrinology 2007;148:4 – 12.

19. Xiang Z, Soto CS, Honig B. Evaluating conformational free energies: the colony energy and its application to the problem of loop prediction. Proc Natl Acad Sci U S A 2002;99:7432 – 7.

20. Van Der Spoel D, Lindahl E, Hess B, Groenhof G, Mark AE, Berendsen HJ. GROMACS: fast, flexible, and free. J Comput Chem 2005;26:1701 – 18.

21. Schuettelkopf AW vAD. PRODRG—a tool for high-throughput crystallography of protein-ligand complexes. Acta Crystallographica 2004;D60:1355 – 63.

22. Izrailev S, Stepaniants S, Balsera M, Oono Y, Schulten K. Molecular dynamics study of unbinding of the avidin-biotin complex. Biophys J 1997;72:1568 – 81.

23. Hamel E. Evaluation of antimitotic agents by quantitative comparisons of their effects on the polymerization of purified tubulin. Cell Biochem Biophys 2003;38:1 – 22.

24. Verdier-Pinard P, Lai JY, Yoo HD, et al. Structure-activity analysis of the interaction of curacin A, the potent colchicine site antimitotic agent, with tubulin and effects of analogs on the growth of MCF-7 breast cancer cells. Mol Pharmacol 1998;53:62 – 76.

25. Mukherjee A, Kirkovsky L, Yao XT, Yates RC, Miller DD, Dalton JT. Enantioselective binding of Casodex to the androgen receptor. Xenobiotica 1996;26:117 – 22.

26. Christiansen RG, Bell MR, D'Ambra TE, et al. Antiandrogenic steroidal sulfonylpyrazoles. J Med Chem 1990;33:2094 – 100.

27. Brzozowski AM, Pike AC, Dauter Z, et al. Molecular basis of agonism and antagonism in the oestrogen receptor. Nature 1997;389:753 – 8.

28. Bourguet W, Ruff M, Chambon P, Gronemeyer H, Moras D. Crystal structure of the ligand-binding domain of the human nuclear receptor RXR-α. Nature 1995;375:377 – 82.

29. Ravelli RB, Gigant B, Curmi PA, et al. Insight into tubulin regulation from a complex with colchicine and a stathmin-like domain. Nature 2004; 428:198 – 202.

30. Lin CM, Ho HH, Pettit GR, Hamel E. Antimitotic natural products combretastatin A-4 and combretastatin A-2: studies on the mechanism of their inhibition of the binding of colchicine to tubulin. Biochemistry 1989; 28:6984 – 91.

31. D'Amato RJ, Lin CM, Flynn E, Folkman J, Hamel E. 2-Methoxyestradiol, an endogenous mammalian metabolite, inhibits tubulin polymerization by interacting at the colchicine site. Proc Natl Acad Sci U S A 1994;91: 3964 – 8.

32. Veldscholte J, Ris-Stalpers C, Kuiper GG, et al. A mutation in the ligand binding domain of the androgen receptor of human LNCaP cells affects steroid binding characteristics and response to anti-androgens. Biochem Biophys Res Commun 1990;173:534 – 40.

33. Gelmann EP. Molecular biology of the androgen receptor. J Clin Oncol 2002;20:3001 – 15.

Molecular Cancer Therapeutics

A bifunctional colchicinoid that binds to the androgen receptor

Nima Sharifi, Ernest Hamel, Markus A. Lill, et al.

Mol Cancer Ther 2007;6:2328-2336.